
Distribution-Aware Reward: Reinforcement Learning over Predictive Distributions for LLM Regression

Jungsoo Park¹, Hyungjoo Chae¹, Ethan Mendes¹, Jay DeYoung²
Varsha Kishore², Wei Xu¹, Alan Ritter¹

¹Georgia Institute of Technology

²Allen Institute for AI


Abstract

Large language models can predict real-valued quantities from heterogeneous inputs such as text, code, and molecular strings, but most training objectives score each decoded floating-point number independently, improving point estimates without ensuring calibrated predictive distributions. This limits applications requiring candidate ranking or uncertainty estimation. We introduce *Distribution-Aware Reward*, an on-policy reinforcement learning objective whose main contribution is to train language models to produce better predictive distributions for regression tasks, rather than only optimizing individual decoded outputs against scalar targets. Our method treats multiple decoded samples as an empirical predictive distribution, evaluates it with the Continuous Ranked Probability Score, and assigns leave-one-out credit based on each rollout’s marginal contribution to distribution quality, rewarding predictions that are both accurate and appropriately dispersed. We evaluate our method on a controlled Gaussian-mixture task, code performance prediction, and molecular property prediction from SMILES strings. Across tasks, our method improves over supervised fine-tuning and pointwise reinforcement learning baselines, with strong rank-correlation gains, including a 6-point Spearman improvement on KBSS. On MoleculeNet, it uses only SMILES strings yet remains competitive with strong graph-based and 3D molecular models. Further analyses show that our method mitigates rollout diversity collapse and improves uncertainty diagnostics, suggesting that directly optimizing predictive distributions makes language model regression more robust and better calibrated.¹

1 Introduction

Many prediction problems in science and engineering are regression tasks, where heterogeneous inputs are mapped to real-valued targets. Recent work has explored large language models (LLMs) as flexible regressors over text, code, and structured descriptions [Requeima et al., 2024, Vacareanu et al., 2024, Song et al., 2024, Tang et al., 2024]. This is useful when inputs are naturally symbolic or textual but the desired output is continuous, such as predicting experimental outcomes from protocols (e.g., reaction yield) [Wu et al., 2018, Park et al., 2025], estimating program performance from source code (e.g., runtime) [Akhauri et al., 2025], or forecasting time series (e.g., weather) [Halawi et al., 2024]. In these settings, LLM regression can support downstream decisions by capturing both magnitude and relative ordering, which classification alone cannot provide.

Current LLM regression methods improve point predictions through in-context learning [Vacareanu et al., 2024], supervised fine-tuning (SFT) [Song et al., 2024, Lukasik et al., 2025], or reinforcement learning (RL) with pointwise numeric rewards [Chen et al., 2025]. However, pointwise rewards optimize each decoded prediction independently, treating rollouts as separate predictions rather than

¹  Code & Data.

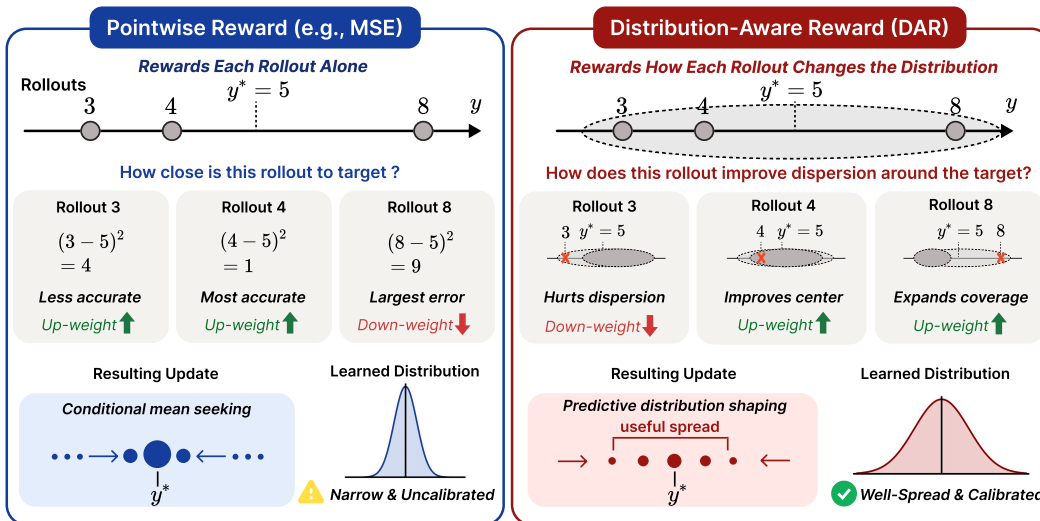


Figure 1: **Pointwise versus distribution-aware reward shaping.** Pointwise MSE reward scores each rollout independently, encouraging predictions to collapse toward the mean. DAR instead scores each rollout by its leave-one-out contribution to the full predictive distribution, rewarding both accuracy and useful spread around the ground truth.

samples from a shared predictive distribution (Figure 1). This discards distributional structure during optimization, even though uncertainty-aware decisions depend not only on a single best estimate but also on how probability mass is distributed across possible values. As a result, pointwise training can yield predictions that are individually close to the target but poorly calibrated, overly narrow, or one-sided as a sampled set. Such behavior weakens uncertainty estimation and rank-based evaluation, since compressed or biased predictions can preserve average error while failing to order examples correctly. This is especially problematic in scientific and applied regression, where downstream decisions depend not only on pointwise error but also on candidate selection, relative ordering, and uncertainty estimation [Gneiting et al., 2007, Gneiting and Raftery, 2007, Levi et al., 2022].

We therefore introduce *Distribution-Aware Reward* (DAR), an RL objective that optimizes the predictive distribution formed by multiple decoded samples. Our main conceptual contribution is to train LLMs for regression by improving the quality of their predictive distributions, rather than only optimizing individual decoded outputs to match scalar targets as in prior methods. Such a view is central to Bayesian regression and probabilistic forecasting [Rasmussen and Williams, 2006, Gneiting and Raftery, 2007], and is closely related to distributional RL, where learning a distribution provides richer training signals than optimizing only its expectation [Bellemare et al., 2017, Puri et al., 2026]. Instead of scoring each rollout in isolation, DAR treats sampled rollouts as an empirical predictive distribution, evaluates the set with the Continuous Ranked Probability Score (CRPS) [Matheson and Winkler, 1976, Gneiting and Raftery, 2007] (a scoring rule for predictive distributions), and uses leave-one-out credit assignment to estimate each rollout’s marginal contribution to distribution quality. This encourages predictions that are accurate and better calibrated as a set (Figure 1), improving both pointwise error and rank correlation.

We evaluate DAR on a Gaussian-mixture synthetic task [Fishkov et al., 2025] and two real-world scientific regression settings: code performance prediction [Akhauri et al., 2025] and MoleculeNet molecular property prediction [Wu et al., 2018]. Across these tasks, DAR improves rank correlation while maintaining comparable or better RMSE; for example, it improves Spearman by 4-6 points over strong baselines on coding regression tasks (KBSS and APPS). It also achieves the strongest Spearman correlation on the synthetic task, better captures extrapolated target structure, and remains competitive on MoleculeNet using only SMILES strings, without graph or 3D molecular representations. Beyond aggregate accuracy, DAR maintains more well-spread rollouts during RL training and yields meaningful uncertainty estimates, with a log-Pearson correlation of 0.91 between rollout standard deviation and prediction error [Levi et al., 2022]. Together, these results show that optimizing predictive distributions improves ranking quality and supports uncertainty estimation, making LLM-based regression more robust.

2 Method

We consider text-conditioned regression, where each input $x \in \mathcal{X}$ is a text serialization of an arbitrary input type. The target $y \in \mathbb{R}$ is a real-valued response. An autoregressive language model with parameters θ defines a conditional distribution over text outputs $\pi_\theta(\mathbf{z} \mid x)$, where each generated output \mathbf{z} is deterministically parsed into a scalar prediction $p = g(\mathbf{z})$. For each training example (x_i, y_i) , we sample K rollouts from the current policy and obtain predictions $\{p_{ik}\}_{k=1}^K$. Training is then driven by rewards computed from these decoded predictions. In this work, we focus on regression reward design in the multi-rollout setting: after briefly introducing common training formulations for LLM regression, we present our distribution-aware reward (DAR), which treats the sampled predictions as an empirical predictive distribution.

2.1 Background: Training Large Language Models for Regression

Recent work has explored large language models as flexible regressors over heterogeneous inputs. Given a training set $\{(x_i, y_i)\}_{i=1}^N$, a standard approach is supervised fine-tuning (SFT). SFT first converts the numeric target y_i into a target text sequence $\mathbf{z}_i^* = (z_{i,1}^*, \dots, z_{i,T_i}^*)$, where each $z_{i,t}^*$ denotes a target token. It then optimizes token-level cross-entropy:

$$\mathcal{L}_{\text{SFT}}(\theta) = - \sum_{i=1}^N \sum_{t=1}^{T_i} \log \pi_\theta(z_{i,t}^* \mid x_i, z_{i,<t}^*). \quad (1)$$

Here, \mathbf{z}_i^* is the textual realization of the target value y_i , such as the string representation of the number. While effective, this objective optimizes the likelihood of a particular answer string rather than a downstream regression metric on the decoded numeric prediction.

Related work has addressed this mismatch by casting regression as classification over a finite grid of numeric candidates [Lukasik et al., 2025]. The model predicts a distribution over predefined values, and the final output is their probability-weighted average. While this preserves cross-entropy-style training, it requires fixing the output discretization in advance, which is less suitable for real-world regression tasks where continuous targets are task-dependent and span different numeric ranges.

An alternative is reinforcement learning (RL), which defines rewards directly on the decoded numeric prediction. For each input x_i , we sample K output sequences from the policy,

$$\mathbf{z}_{ik} \sim \pi_\theta(\cdot \mid x_i), \quad p_{ik} = g(\mathbf{z}_{ik}), \quad k = 1, \dots, K, \quad (2)$$

where \mathbf{z}_{ik} denotes the k -th sampled text sequence and $g(\cdot)$ parses the generated text into a real-valued prediction $p_{ik} \in \mathbb{R}$. We then assign a scalar reward $R_{ik} = R(p_{ik}, y_i)$ based on the predicted value and the target.

A natural pointwise baseline is an MSE-style reward [Koa et al., 2025, Chen et al., 2025],

$$R_{ik}^{\text{MSE}} = -(p_{ik} - y_i)^2, \quad (3)$$

which scores each sampled prediction according to its own regression error. Compared with SFT, this formulation allows optimization to operate directly on the decoded numeric output rather than token-level cross-entropy supervision.

However, pointwise rewards² only evaluate whether each individual rollout is close to the target. They do not evaluate whether the set of sampled predictions for an input, $\{p_{ik}\}_{k=1}^K$, forms a useful predictive distribution. As a result, a model can improve pointwise accuracy while still producing samples that are poorly calibrated, overly narrow, or one-sided.

This distinction matters because sampled predictions are often used not only as individual numeric outputs, but also as an empirical distribution that represents uncertainty. If training rewards only favor isolated closeness to the target, the rollout set may fail to capture meaningful dispersion around plausible target values. Such compressed or miscalibrated predictions can also hurt rank-based evaluation: even when average error is reasonable, insufficient variation across examples can make it difficult to correctly order candidates by predicted value. This motivates DAR. Instead of rewarding each sampled prediction in isolation, we treat the K rollouts as an empirical predictive distribution and design training feedback to improve the quality of that distribution directly.

²We refer to rewards that score each sampled prediction independently, such as rollout-level MSE, as pointwise rewards.

2.2 Distribution-Aware Reward (DAR): CRPS with Leave-One-Out Credit Assignment

To move beyond isolated point errors, we propose a distribution-aware reward (DAR) that optimizes the rollout-induced predictive distribution. For each input x_i , the K predictions $\{p_{ik}\}_{k=1}^K$ define an empirical predictive distribution F_i . We evaluate F_i against the target y_i using the Continuous Ranked Probability Score (CRPS), a proper scoring rule for predictive distributions [Matheson and Winkler, 1976, Gneiting and Raftery, 2007]. Since CRPS is conventionally minimized, we use its negated empirical form as a maximization reward:

$$S_i = -\text{CRPS}(F_i, y_i) = -\frac{1}{K} \sum_{k=1}^K |p_{ik} - y_i| + \frac{1}{2K^2} \sum_{k=1}^K \sum_{\ell=1}^K |p_{ik} - p_{i\ell}|. \quad (4)$$

Higher S_i indicates a better predictive distribution. The first term rewards concentration of probability mass near the target, while the second term prevents the empirical distribution from becoming overly degenerate by accounting for pairwise dispersion among rollouts. Together, these terms favor predictive distributions that are accurate without collapsing all probability mass onto a single point estimate.

On-policy optimization requires a scalar reward for each rollout, while the score in Eq. 4 is defined for the full predictive distribution induced by the sampled set. We therefore convert this distribution-level score into rollout-level feedback by measuring the marginal contribution of each rollout. For input x_i , let F_i denote the empirical distribution of $\{p_{i1}, \dots, p_{iK}\}$ and let $S_i = -\text{CRPS}(F_i, y_i)$. For rollout p_{ik} , let $F_i^{(-k)}$ be the leave-one-out empirical distribution obtained by removing p_{ik} , and let $S_i^{(-k)} = -\text{CRPS}(F_i^{(-k)}, y_i)$. We define the rollout-level DAR reward as the leave-one-out marginal contribution:

$$R_{ik}^{\text{DAR}} = S_i - S_i^{(-k)}. \quad (5)$$

If removing p_{ik} lowers the negated CRPS score, then $R_{ik}^{\text{DAR}} > 0$, meaning that the rollout improves the predictive distribution. If removing it increases the score, then $R_{ik}^{\text{DAR}} < 0$, meaning that the rollout is harmful or redundant. Unlike pointwise rewards, DAR explicitly attributes credit based on how each rollout affects the *set* of predictions, encouraging predictive sets that are well-centered and appropriately dispersed.

Running example: MSE vs. DAR. We illustrate that DAR can upweight a rollout with larger pointwise error when it improves the *collective* predictive distribution. Consider a single input with target $y = 5$ and three rollouts producing predictions $[3, 4, 8]$ (Figure 1). A pointwise MSE-based reward scores rollouts independently and therefore favors 4 (lowest error) and 3, while penalizing 8, encouraging concentration around near-target values.

DAR instead scores the *set* of rollouts via CRPS and assigns credit by marginal contribution. Here, 3 and 4 place mass on the same side of y , yielding a biased and under-dispersed predictive set; the rollout 8, though less accurate individually, increases spread and reduces degeneracy. Thus, removing 8 can worsen CRPS more than removing a redundant near-target rollout, giving higher R_{ik}^{DAR} for 8 and lower R_{ik}^{DAR} for a redundant rollout 3.

3 Experimental Setup

We evaluate whether regression-trained LLMs can serve as *polyfunctional regressors* across heterogeneous settings that differ in input modality and supervision. Our evaluation includes one synthetic regression task designed to probe interpolation and extrapolation behavior, as well as two real-world scientific regression tasks. Additional details of the experimental setup, including task prompts and examples, are provided in Appendix B and Appendix H, respectively.

3.1 Tasks

Synthetic Distributional Regression. We use a controlled synthetic task where the target is sampled from a known heteroscedastic two-component Gaussian mixture conditioned on a scalar input x [Fishkov et al., 2025]. We train on 1,200 samples from the ground-truth process and evaluate on disjoint test regions with 600 samples covering both interpolation and extrapolation. We report square-root MSE (RMSE) and Spearman correlation.

Coding Performance Prediction. We study real-world scientific regression tasks where the input is source code, either a Triton kernel or a Python implementation, and the target is a real-valued performance metric [Akhaoui et al., 2025]. Specifically, we consider (i) Triton kernel latency prediction and (ii) Python peak-memory prediction, using random train/validation/test splits of 6K/1K/1K examples. Following the original setup, we report Spearman correlation and MAE.

Molecular Property Prediction. We also evaluate on MoleculeNet regression tasks [Wu et al., 2018], where the input is a SMILES string [Weininger, 1988] and the target is a real-valued molecular property. Specifically, FreeSolv predicts hydration free energy, ESOL predicts aqueous solubility, and Lipophilicity predicts a logD/logP-style measure of hydrophobicity. For example, given the SMILES string CCO for ethanol, the model predicts a continuous property value such as its aqueous solubility. This setting represents a classical scientific regression regime where strong non-LLM baselines have historically used graph-based molecular representations. We use the official scaffold split [Zhou et al., 2023] and report RMSE following the standard setup.

3.2 Implementation Details

We follow a standard on-policy RL fine-tuning recipe for sequence models [Schulman et al., 2017, Ouyang et al., 2022]. Unless otherwise stated, we use a learning rate of 1×10^{-6} , train for up to 300 steps, and sample $K = 12$ rollouts per input with temperature 1.0 for exploration. All RL and SFT experiments are implemented in ver1 [Sheng et al., 2024], with KL regularization applied in the loss against the fixed reference policy, initialized from the same checkpoint used to start RL training. We select the checkpoint with the best validation performance and report its test results.

For the synthetic experiment, we use Qwen2.5-0.5B-Instruct [Qwen Team, 2024]; for real regression tasks, we use Qwen3-4B-Instruct as the default backbone [Yang et al., 2025]. We disable explicit reasoning by default for efficiency and analyze its effect in Appendix C. During training, each rollout is parsed into a scalar prediction using a strict output format. Invalid rollouts receive method-specific penalties, such as the minimum batch reward for the negative-MSE baseline. At evaluation time, we generate 32 samples and average them as the final prediction, following standard LLM regression practice [Lukasik et al., 2024, 2025, Akhaoui et al., 2025]. We repeat evaluation with 5 random seeds and report averaged metrics [Chen et al., 2025].

3.3 Baselines

We compare against baselines that cover the main ways LLMs can be used for regression. At the prompting level, we evaluate both proprietary frontier LLMs and the open-weight base model in *ICL* settings [Vacareanu et al., 2024], capturing off-the-shelf inference without task-specific training. We also evaluate domain-specific LLMs, such as ChemLLM [Zhang et al., 2024, Yu et al., 2024], in the zero-shot setting.

At the training level, we consider a value-head regression baseline trained with MSE [Tang et al., 2024] and an SFT baseline that fine-tunes the model to generate a single numeric output [Lukasik et al., 2025]. Finally, in the on-policy RL setting, we compare conventional pointwise reward optimization based on negative MSE [Chen et al., 2025] against DAR, which directly optimizes the predictive distribution induced by multiple rollouts.

4 Experimental Results

We evaluate DAR across a controlled synthetic task and two real-world scientific regression settings. The synthetic 1D regression task allows us to visually inspect how different objectives capture nonlinear target structure, while the real-world tasks measure practical performance using standard pointwise and rank-based metrics.

4.1 Synthetic Distributional Regression

Figure 2 compares SFT, MSE reward shaping, a Neural Gaussian Ensemble [Fishkov et al., 2025], and DAR on the synthetic 1D Gaussian mixture task. DAR achieves the highest Spearman correlation among the LLM-based methods, indicating that it better preserves the global ordering of the target

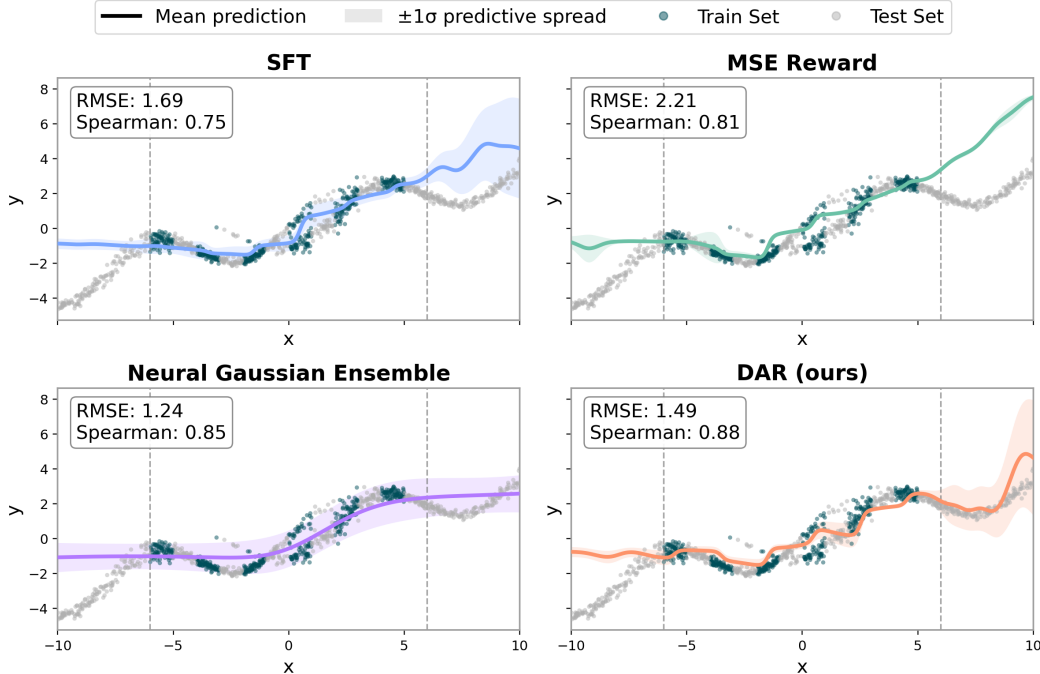


Figure 2: **Synthetic distributional regression.** Mean predictions and $\pm 1\sigma$ predictive spread on the 1D Gaussian mixture task. Dashed vertical lines at $x = \pm 6$ mark the boundary between interpolation and extrapolation regions.

function. Qualitatively, it also follows the target structure more closely, especially in the extrapolation region (6, 10). In contrast, SFT and MSE reward shaping show larger deviations, and all neural baselines struggle in the harder extrapolation region $[-10, -6]$.

The Neural Gaussian Ensemble obtains lower RMSE, which is expected because it is a dedicated Gaussian neural model with an inductive bias well matched to this synthetic distribution. However, even without task-specific inductive biases or parametric assumptions, DAR adapts well to the extrapolation setting and demonstrates strong rank correlation. This demonstrates the value of directly optimizing the predictive distribution. Note that this experiment is not intended to show that DAR is specialized for Gaussian mixtures, but rather to use a controlled nonlinear setting to inspect how distribution-aware optimization changes the learned prediction structure.

4.2 Performance Prediction

Table 1 reports code-to-performance prediction results, where DAR achieves the strongest overall performance.³ In particular, DAR obtains the best rank correlation and competitive or lower MAE, showing that distribution-aware reward optimization improves code performance prediction beyond standard SFT and pointwise RL rewards. The gains are especially clear in Spearman correlation, suggesting better sensitivity to input-dependent variation and more reliable ranking of examples.

Off-the-shelf ICL performs poorly, indicating that general-purpose LLMs do not reliably map source code to precise continuous performance metrics without task-specific adaptation. This is expected because latency and memory depend on fine-grained implementation details that are difficult to infer from prompting alone. The value-head baseline also underperforms, suggesting that simply attaching a regression head to LLM representations is not sufficient for these long context tasks. SFT substantially improves performance once task-specific supervision is provided, but DAR further improves over SFT by directly optimizing the predictive distribution. In contrast, pointwise MSE reward shaping can sometimes produce collapsed, low-variance predictions, reflecting the mean-seeking behavior of instance-wise error minimization.

³Results from Akhauri et al. [2025] use the original paper’s split; we use a different split on the same dataset.

Model	Method	KBSS (latency)		APPS (memory)	
		ρ (\uparrow)	MAE (\downarrow)	ρ (\uparrow)	MAE (\downarrow)
Qwen3-30B-A3B RLM	ICL [Vacareanu et al., 2024]	0.32	0.027	0.38	1.10e4
	SFT [Akhauri et al., 2025]	0.51	–	0.93	–
Qwen3-4B	ICL [Vacareanu et al., 2024]	0.23	0.019	0.27	3.46e8
Qwen3-4B	Value Head [Tang et al., 2024]	0.23	0.025	0.65	306
Qwen3-4B	SFT [Lukasik et al., 2025]	0.61	0.013	0.93	29.5
Qwen3-4B	MSE [Chen et al., 2025]	0.60	0.012	0.92	29.8
Qwen3-4B	DAR (ours)	0.66[†]	0.011	0.96[†]	29.1[†]

Table 1: **Code performance prediction.** Results on KBSS latency prediction and APPS peak-memory prediction. KBSS MAE is reported in milliseconds, and APPS MAE is reported in 10^3 bytes. [†] denotes statistically significant improvement over the strongest baseline under paired bootstrap testing ($p < 0.05$).

Model	Method	ESOL	FreeSolv	Lipo
		RMSE (\downarrow)	RMSE (\downarrow)	RMSE (\downarrow)
D-MPNN	GNN [Yang et al., 2019]	1.050	2.082	0.683
AttentiveFP	Graph attention [Xiong et al., 2020]	0.877	2.073	0.721
Uni-Mol	3D molecular representation [Zhou et al., 2023]	0.788	1.480	0.603
Qwen3-30B-A3B	ICL [Vacareanu et al., 2024]	1.886	4.160	1.427
Mol-Instructions	Molecular instruction [Fang et al., 2023]	2.271	6.891	1.691
ChemLLM	Chemical LLM [Zhang et al., 2024]	1.946	10.452	1.797
LlaSMol	Molecular LLM [Yu et al., 2024]	1.150	7.150	1.010
Qwen3-4B	ICL [Vacareanu et al., 2024]	2.133	4.368	1.284
Qwen3-4B	Value Head [Tang et al., 2024]	0.893	3.460	0.946
Qwen3-4B	SFT [Lukasik et al., 2025]	0.881	2.755	0.820
Qwen3-4B	MSE [Chen et al., 2025]	0.878	2.561	0.822
Qwen3-4B	DAR (ours)	0.871	2.360[†]	0.776[†]

Table 2: **Molecular property prediction.** RMSE on MoleculeNet regression tasks. ESOL is measured in log molar solubility, FreeSolv in kcal/mol hydration free energy, and Lipophilicity in logD. Graph and molecular ML baselines use task-specific molecular representations, while the LLM methods use only SMILES strings. [†] denotes statistically significant improvement over the strongest LLM baseline under paired bootstrap testing ($p < 0.05$).

4.3 Molecule Property Prediction

Table 2 reports MoleculeNet property prediction results. Graph-based and 3D molecular models remain strong baselines because they use chemistry-aware representations, including atom-bond graph structure, curated molecular features, or geometric information [Yang et al., 2019, Xiong et al., 2020, Zhou et al., 2023]. In contrast, the LLM methods operate only on SMILES strings, which provide a textual representation of molecular structure without explicit graph or 3D inductive biases.

Despite this disadvantage, regression fine-tuning substantially improves LLM performance. DAR consistently outperforms other LLM training strategies and achieves statistically significant gains on FreeSolv and Lipophilicity. MSE reward shaping also improves over SFT in some cases, but DAR gives the strongest overall results, suggesting that distribution-level optimization provides more reliable regression behavior than pointwise objectives alone. Again, the ICL [Vacareanu et al., 2024] and value-head fine-tuning [Tang et al., 2024] approaches underperform compared to SFT, MSE, and DAR. This may be because ICL explores the training data only through a small set of prompts, while value-head fine-tuning requires randomly initialized numeric prediction modules that may be difficult to train effectively.

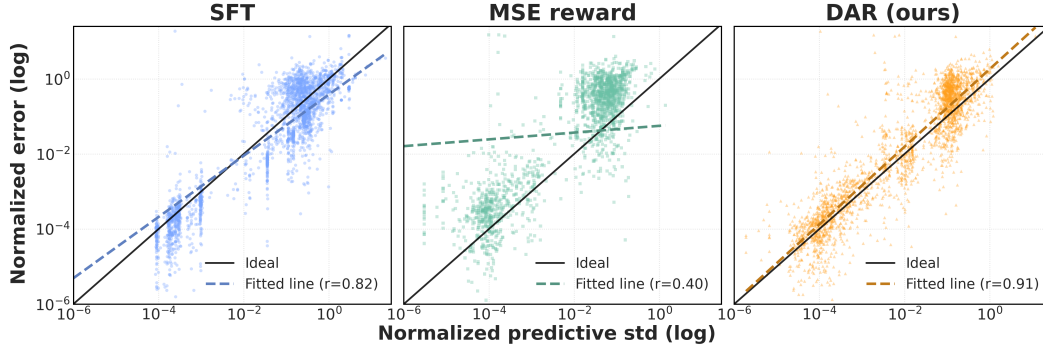


Figure 3: **Distribution-level calibration and uncertainty diagnostics.** We compare predictive distributions from SFT, MSE reward shaping, and DAR. The plots show normalized predictive standard deviation versus normalized prediction error on a log-log scale, along with fitted trends and the ideal diagonal. DAR achieves stronger standard deviation-error alignment, indicating more informative rollout dispersion and better predictive distribution quality.

5 Analysis

This section analyzes how distribution-aware reward shaping affects the predictive distributions produced by LLM regression models. Beyond aggregate pointwise metrics, we examine whether rollout distributions provide meaningful uncertainty estimates at evaluation time, remain diverse during training, and cover the ground-truth values.

5.1 Predictive Uncertainty from Rollout Dispersion

In probabilistic regression, dispersion across predictions is commonly used as a proxy for predictive uncertainty [Rasmussen and Williams, 2006, Lakshminarayanan et al., 2017, Kendall and Gal, 2017]. We therefore evaluate whether the rollout distribution produced by each method provides useful uncertainty information, rather than only accurate point estimates. For each prompt, we use the mean of sampled predictions as the point estimate and the standard deviation of sampled predictions as the predictive uncertainty score.

Figure 3 presents complementary distribution-level diagnostics. We compare the normalized predictive standard deviation against the normalized prediction error on a log-log scale, using prediction examples from all five datasets. A useful uncertainty estimate should assign larger uncertainty to examples with larger realized errors, so stronger alignment with the ideal diagonal indicates more informative uncertainty estimates. DAR shows the strongest log-scale correlation between predictive standard deviation and prediction error, suggesting that its rollout dispersion better reflects example-level prediction difficulty. In contrast, SFT and MSE exhibit weaker alignment. SFT tends to produce overly diffuse uncertainty, while MSE reward shaping can result in less informative predictive spread. Overall, these results suggest that directly optimizing distribution-level rewards helps the model produce predictive distributions whose uncertainty is better calibrated to actual errors. We further observe consistent improvements in non-parametric scoring functions for evaluating predictive distribution quality, as reported in Appendix D.

5.2 Distribution of Rollouts During Training

To illustrate how distribution-aware reward shaping changes training dynamics, we analyze rollout behavior during GRPO [Shao et al., 2024] training, motivated by prior work showing that RL fine-tuning can reduce output diversity or policy entropy [Kirk et al., 2024, Cui et al., 2025]. For each input i with rollout predictions $p_{i1:K}$ and target y_i , we measure the bracket rate, defined as $\mathbb{I}(\min_k p_{ik} \leq y_i \leq \max_k p_{ik})$, which checks whether the decoded predictions span the ground-truth value. We also track token-level policy entropy from GRPO training, measuring how much stochasticity remains in the next-token distribution. Together, bracket rate captures target-covering prediction diversity, while policy entropy captures collapse toward deterministic outputs.

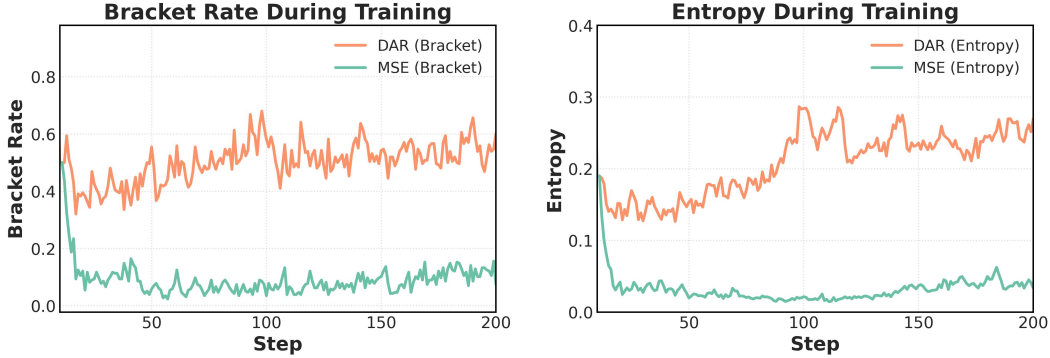


Figure 4: **Training dynamics during RL under DAR (ours) and MSE reward shaping.** Bracket rate measures the fraction of examples whose rollout set contains predictions on both sides of the ground truth, while entropy measures prediction diversity.

Figure 4 summarizes KBSS training results with Qwen3-4B-Instruct. The left plot shows that DAR achieves a higher bracketing rate than the MSE reward baseline, indicating that its rollouts more often cover the ground-truth value. The right plot further shows that DAR maintains higher rollout entropy during training, suggesting that it mitigates diversity collapse under GRPO. Together, these results suggest that distribution-aware reward shaping encourages a more useful form of exploration: predictive samples remain diverse while better spanning the target, leading to higher-quality predictive distributions than pointwise MSE reward shaping.

6 Related Work

LLMs Regression. Recent work shows that LLMs can act as flexible regressors over heterogeneous inputs via direct numeric prediction, in-context regression, and embedding-based regression or optimization [Song et al., 2024, Vacareanu et al., 2024, Nguyen et al., 2024, Tang et al., 2024, Yuchi et al., 2026]. Other studies adapt autoregressive LLMs more directly for regression, including regression-aware inference over discretized numeric candidates [Lukasik et al., 2024], regression-aware fine-tuning [Lukasik et al., 2025], chain-of-thought regression for judge-style tasks [Chiang et al., 2025], and reinforcement learning for decoding-based regression [Chen et al., 2025]. Recent benchmarks further stress-test LLM regression in realistic settings such as code-to-metric prediction, multi-step textual regression, and forecasting LLM benchmark scores from task and configuration descriptions [Akhauri et al., 2025, Tchuindjo and Khattab, 2025, Park et al., 2025]. We build on this direction by studying on-policy RL with a distribution-aware reward.

RL for Forecasting and Distribution-Aware Reward Design. RL fine-tuning for numeric prediction with LLMs has been studied mainly in forecasting, where rewards often target temporal reasoning, outcome accuracy, or calibration [Luo et al., 2025, Koa et al., 2025, Turtel et al., 2025, Chandak et al., 2025]. In contrast, we study *non-temporal* scalar regression and directly optimize the empirical predictive distribution induced by multiple numeric rollouts. Our leave-one-out credit assignment is related to RLOO-style estimators [Kool et al., 2019, Ahmadian et al., 2024], but serves a different purpose. RLOO uses leave-one-out rewards mainly as a baseline for advantage estimation, whereas DAR uses leave-one-out scoring to define each rollout’s marginal contribution to distribution quality. DAR is also distinct from ranking-based objectives [Burges et al., 2005, Joachims, 2002], which optimize relative orderings rather than calibrated numeric predictive distributions.

7 Conclusion

We introduced DAR, a distribution-aware RL objective that optimizes the predictive distribution formed by multiple LLM rollouts. Across synthetic and real-world scientific regression tasks, DAR improves rank-based performance while maintaining competitive or better pointwise error. Distribution-level analyses show better prediction diversity and calibration metrics, suggesting that predictive-distribution optimization is a promising direction for LLM-based scientific regression.

Acknowledgements

This research is supported in part by the NSF under grant numbers IIS-2052498, SMA-2418946, and NAIRR250217, in addition to a gift from Google. Any opinions, findings, and conclusions or recommendations expressed in this material are those of the author(s) and do not necessarily reflect the views of the National Science Foundation.

References

- Arash Ahmadian, Chris Cremer, Matthias Gallé, Marzieh Fadaee, Julia Kreutzer, Olivier Pietquin, Ahmet Üstün, and Sara Hooker. Back to basics: Revisiting reinforce style optimization for learning from human feedback in llms. In *Proceedings of the 62nd Annual Meeting of the Association for Computational Linguistics (Volume 1: Long Papers)*, 2024. URL <https://aclanthology.org/2024.acl-long.662/>.
- Yash Akhauri, Xingyou Song, Arissa Wongpanich, Bryan Lewandowski, and Mohamed S. Abdelfattah. Regression language models for code. *arXiv preprint arXiv:2509.26476*, 2025. URL <https://arxiv.org/abs/2509.26476>.
- Marc G. Bellemare, Will Dabney, and Rémi Munos. A distributional perspective on reinforcement learning. In *Proceedings of the 34th International Conference on Machine Learning*, pages 449–458. PMLR, 2017.
- Johannes Bracher, Evan L. Ray, Tilmann Gneiting, and Nicholas G. Reich. Evaluating epidemic forecasts in an interval format. *PLOS Computational Biology*, 17(2):e1008618, 2021. doi: 10.1371/journal.pcbi.1008618.
- Christopher Burges, Tal Shaked, Erin Renshaw, Ari Lazier, Matt Deeds, Nicole Hamilton, and Greg Hullender. Learning to rank using gradient descent. In *Proceedings of the 22nd International Conference on Machine Learning*, pages 89–96, 2005.
- Nikhil Chandak, Shashwat Goel, Ameeya Prabhu, Moritz Hardt, and Jonas Geiping. Scaling open-ended reasoning to predict the future. *arXiv preprint arXiv:2512.25070*, 2025. URL <https://arxiv.org/abs/2512.25070>.
- Ming Chen, Sheng Tang, Rong-Xi Tan, Ziniu Li, Jiacheng Chen, Ke Xue, and Chao Qian. Beyond token-level supervision: Unlocking the potential of decoding-based regression via reinforcement learning. *arXiv preprint arXiv:2512.06533*, 2025.
- Cheng-Han Chiang, Hung-yi Lee, and Michal Lukasik. TRACT: Regression-aware fine-tuning meets chain-of-thought reasoning for LLM-as-a-judge. In Wanxiang Che, Joyce Nabende, Ekaterina Shutova, and Mohammad Taher Pilehvar, editors, *Proceedings of the 63rd Annual Meeting of the Association for Computational Linguistics (Volume 1: Long Papers)*, pages 2934–2952, Vienna, Austria, July 2025. Association for Computational Linguistics. URL <https://aclanthology.org/2025.acl-long.147/>.
- Ganqu Cui, Yuchen Zhang, Jiacheng Chen, Lifan Yuan, Zhi Wang, Yuxin Zuo, Haozhan Li, Yuchen Fan, Huayu Chen, Weize Chen, Zhiyuan Liu, Hao Peng, Lei Bai, Wanli Ouyang, Yu Cheng, Bowen Zhou, and Ning Ding. The entropy mechanism of reinforcement learning for reasoning language models. *arXiv preprint arXiv:2505.22617*, 2025. URL <https://arxiv.org/abs/2505.22617>.
- Yin Fang, Xiaozhuan Liang, Ningyu Zhang, Kangwei Liu, Rui Huang, Zhuo Chen, Xiaohui Fan, and Huajun Chen. Mol-instructions: A large-scale biomolecular instruction dataset for large language models. *arXiv preprint arXiv:2306.08018*, 2023.
- Alexander Fishkov, Kajetan Schweighofer, Mykyta Ielanskyi, Nikita Kotelevskii, Mohsen Guizani, and Maxim Panov. Uncertainty quantification for regression using proper scoring rules. *arXiv preprint arXiv:2509.26610*, 2025.
- Tilmann Gneiting. Making and evaluating point forecasts. *Journal of the American Statistical Association*, 106(494):746–762, 2011. doi: 10.1198/jasa.2011.r10138.

- Tilman Gneiting and Adrian E Raftery. Strictly proper scoring rules, prediction, and estimation. *Journal of the American Statistical Association*, 102(477):359–378, 2007.
- Tilman Gneiting, Fadoua Balabdaoui, and Adrian E. Raftery. Probabilistic forecasts, calibration and sharpness. *Journal of the Royal Statistical Society: Series B (Statistical Methodology)*, 69(2): 243–268, 2007.
- Danny Halawi, Fred Zhang, Yueh-Han Chen, and Jacob Steinhardt. Approaching human-level forecasting with language models. In *Advances in Neural Information Processing Systems (NeurIPS)*, 2024. URL https://proceedings.neurips.cc/paper_files/paper/2024/file/5a5acfd0876c940d81619c1dc60e7748-Paper-Conference.pdf.
- Andre Wang He, Daniel Fried, and Sean Welleck. Rewarding the unlikely: Lifting grpo beyond distribution sharpening. In *Proceedings of the 2025 Conference on Empirical Methods in Natural Language Processing*, pages 25559–25571, 2025.
- Thorsten Joachims. Optimizing search engines using clickthrough data. In *Proceedings of the Eighth ACM SIGKDD International Conference on Knowledge Discovery and Data Mining*, pages 133–142, 2002.
- Alex Kendall and Yarin Gal. What uncertainties do we need in bayesian deep learning for computer vision? In *Advances in Neural Information Processing Systems*, volume 30. Curran Associates, Inc., 2017.
- Robert Kirk, Ishita Mediratta, Christoforos Nalmpantis, Jelena Luketina, Eric Hambro, Edward Grefenstette, and Roberta Raileanu. Understanding the effects of RLHF on LLM generalisation and diversity. In *International Conference on Learning Representations*, 2024. URL <https://openreview.net/forum?id=PXD3FAVHJT>.
- Kelvin JL Koa, Jan Chen, Yunshan Ma, Huanhuan Zheng, and Tat-Seng Chua. Reasoning on time-series for financial technical analysis. *arXiv preprint arXiv:2511.08616*, 2025. URL <https://arxiv.org/abs/2511.08616>.
- Wouter Kool, Herke van Hoof, and Max Welling. Buy 4 reinforce samples, get a baseline for free! In *Deep Reinforcement Learning Meets Structured Prediction Workshop at ICLR*, 2019. URL <https://openreview.net/forum?id=r1lgTGL5DE>.
- Balaji Lakshminarayanan, Alexander Pritzel, and Charles Blundell. Simple and scalable predictive uncertainty estimation using deep ensembles. In *Advances in Neural Information Processing Systems*, volume 30. Curran Associates, Inc., 2017.
- Dan Levi, Liran Gispan, Niv Giladi, and Ethan Fetaya. Evaluating and calibrating uncertainty prediction in regression tasks. *Sensors*, 22(15):5540, 2022. doi: 10.3390/s22155540.
- Michal Lukasik, Harikrishna Narasimhan, Aditya Krishna Menon, Felix Yu, and Sanjiv Kumar. Regression aware inference with llms. In *Findings of the Association for Computational Linguistics: EMNLP 2024*, pages 13667–13678, 2024. doi: 10.18653/v1/2024.findings-emnlp.799. URL <https://aclanthology.org/2024.findings-emnlp.799/>.
- Michal Lukasik, Zhao Meng, Harikrishna Narasimhan, Yin-Wen Chang, Aditya Krishna Menon, Felix Yu, and Sanjiv Kumar. Better autoregressive regression with LLMs via regression-aware fine-tuning. In *The Thirteenth International Conference on Learning Representations*, 2025. URL <https://openreview.net/forum?id=xGs7Ch3Vyo>.
- Yucong Luo, Yitong Zhou, Mingyue Cheng, Jiahao Wang, Daoyu Wang, Tingyue Pan, and Jintao Zhang. Time series forecasting as reasoning: A slow-thinking approach with reinforced llms. *arXiv preprint arXiv:2506.10630*, 2025. URL <https://arxiv.org/abs/2506.10630>.
- James E. Matheson and Robert L. Winkler. Scoring rules for continuous probability distributions. *Management Science*, 22(10):1087–1096, 1976.
- Tung Nguyen, Qiuyi Zhang, Bangding Yang, Chansoo Lee, Jorg Bornschein, Yingjie Miao, Sagi Perel, Yutian Chen, and Xingyou Song. Predicting from strings: Language model embeddings for bayesian optimization. *arXiv preprint arXiv:2410.10190*, 2024. URL <https://arxiv.org/abs/2410.10190>.

- Long Ouyang, Jeffrey Wu, Xu Jiang, Diogo Almeida, Carroll Wainwright, Pamela Mishkin, Chong Zhang, Sandhini Agarwal, Katarina Slama, Alex Ray, et al. Training language models to follow instructions with human feedback. *arXiv preprint arXiv:2203.02155*, 2022. URL <https://arxiv.org/abs/2203.02155>.
- Jungsoo Park, Ethan Mendes, Gabriel Stanovsky, and Alan Ritter. Anticipatory evaluation of language models. *arXiv preprint arXiv:2509.20645*, 2025. doi: 10.48550/arXiv.2509.20645. URL <https://arxiv.org/abs/2509.20645>.
- Aleksei Petrenko, Ben Lipkin, Kevin Chen, Erik Wijmans, Marco Cusumano-Towner, Raja Giryes, and Philipp Krähenbühl. Entropy-preserving reinforcement learning. *arXiv preprint arXiv:2603.11682*, 2026.
- Isha Puri, Mehul Damani, Idan Shenfeld, Marzyeh Ghassemi, Jacob Andreas, and Yoon Kim. Reaching beyond the mode: RL for distributional reasoning in language models. *arXiv preprint arXiv:2603.24844*, 2026.
- Qwen Team. Qwen2 technical report. *arXiv preprint arXiv:2407.10671*, 2024. URL <https://arxiv.org/abs/2407.10671>.
- Carl Edward Rasmussen and Christopher K. I. Williams. *Gaussian Processes for Machine Learning*. Adaptive Computation and Machine Learning. MIT Press, 2006. ISBN 026218253X.
- James Requeima, John Bronskill, Dami Choi, Richard Turner, and David K. Duvenaud. Llm processes: Numerical predictive distributions conditioned on natural language. In *Advances in Neural Information Processing Systems (NeurIPS)*, volume 37, pages 109609–109671, 2024.
- John Schulman, Filip Wolski, Prafulla Dhariwal, Alec Radford, and Oleg Klimov. Proximal policy optimization algorithms. *arXiv preprint arXiv:1707.06347*, 2017. URL <https://arxiv.org/abs/1707.06347>.
- Zhihong Shao, Peiyi Wang, Qihao Zhu, Runxin Xu, Junxiao Song, Xiao Bi, Haowei Zhang, Mingchuan Zhang, Y. K. Li, Y. Wu, and Daya Guo. Deepseekmath: Pushing the limits of mathematical reasoning in open language models. *arXiv preprint arXiv:2402.03300*, 2024. doi: 10.48550/arXiv.2402.03300. URL <https://arxiv.org/abs/2402.03300>.
- Guangming Sheng, Chi Zhang, Zilingfeng Ye, Xibin Wu, Wang Zhang, Ru Zhang, Yanghua Peng, Haibin Lin, and Chuan Wu. Hybridflow: A flexible and efficient rlhf framework. *arXiv preprint arXiv:2409.19256*, 2024. doi: 10.48550/arXiv.2409.19256. URL <https://arxiv.org/abs/2409.19256>.
- Xingyou Song, Oscar Li, Chansoo Lee, Bangding Yang, Daiyi Peng, Sagi Perel, and Yutian Chen. Omnipred: Language models as universal regressors. *arXiv preprint arXiv:2402.14547*, 2024. URL <https://arxiv.org/abs/2402.14547>.
- Eric Tang, Bangding Yang, and Xingyou Song. Understanding llm embeddings for regression. *arXiv preprint arXiv:2411.14708*, 2024. URL <https://arxiv.org/abs/2411.14708>.
- Diane Tchuindjo and Omar Khattab. Reasoning-intensive regression. *arXiv preprint arXiv:2508.21762*, 2025. URL <https://arxiv.org/abs/2508.21762>.
- Benjamin Turtel, Danny Franklin, Kris Skotheim, Luke Hewitt, and Philipp Schoenegger. Outcome-based reinforcement learning to predict the future. *arXiv preprint arXiv:2505.17989*, 2025. URL <https://arxiv.org/abs/2505.17989>.
- Robert Vacareanu, Vlad-Andrei Negru, Vasile Suciuc, and Mihai Surdeanu. From words to numbers: Your large language model is secretly a capable regressor when given in-context examples. *CoRR*, 2024.
- Jason Wei, Xuezhi Wang, Dale Schuurmans, Maarten Bosma, Fei Xia, Ed Chi, Quoc V. Le, Denny Zhou, et al. Chain-of-thought prompting elicits reasoning in large language models. In *Advances in Neural Information Processing Systems (NeurIPS)*, volume 35, pages 24824–24837, 2022.

- David Weininger. Smiles, a chemical language and information system. 1. introduction to methodology and encoding rules. *Journal of Chemical Information and Computer Sciences*, 28(1):31–36, 1988. doi: 10.1021/ci00057a005.
- Zhenqin Wu, Bharath Ramsundar, Evan N. Feinberg, Joseph Gomes, Caleb Geniesse, Aneesh S. Pappu, Karl Leswing, and Vijay Pande. Moleculenet: a benchmark for molecular machine learning. *Chemical Science*, 9(2):513–530, 2018. doi: 10.1039/C7SC02664A.
- Zhaoping Xiong, Dingyan Wang, Xin Liu, Feisheng Zhong, Xiaohong Wan, Xutong Li, Zhaojun Li, Xiaoqin Luo, Kun Chen, Hualiang Jiang, and Mingyue Zheng. Pushing the boundaries of molecular representation for drug discovery with the graph attention mechanism. *Journal of Medicinal Chemistry*, 63(16):8749–8760, 2020. doi: 10.1021/acs.jmedchem.9b00959.
- An Yang, Anfeng Li, Baosong Yang, Beichen Zhang, Binyuan Hui, Bo Zheng, Bowen Yu, Chang Gao, Chengen Huang, Chenxu Lv, et al. Qwen3 technical report. *arXiv preprint arXiv:2505.09388*, 2025. URL <https://arxiv.org/abs/2505.09388>.
- Kevin Yang, Kyle Swanson, Wengong Jin, Connor Coley, Philip Eiden, Hua Gao, Angelica Guzman-Perez, Timothy Hopper, Brian Kelley, Miriam Mathea, Alex Palmer, Volker Settels, Tommi Jaakkola, Klavs F. Jensen, and Regina Barzilay. Analyzing learned molecular representations for property prediction. *Journal of Chemical Information and Modeling*, 59(8):3370–3388, 2019. doi: 10.1021/acs.jcim.9b00237.
- Botao Yu, Frazier N Baker, Ziqi Chen, Xia Ning, and Huan Sun. Lllmol: Advancing large language models for chemistry with a large-scale, comprehensive, high-quality instruction tuning dataset. *arXiv preprint arXiv:2402.09391*, 2024.
- Fengting Yuchi, Li Du, and Jason Eisner. Lllms know more about numbers than they can say. In *Proceedings of the 19th Conference of the European Chapter of the Association for Computational Linguistics (Volume 2: Short Papers)*, pages 659–673, 2026.
- Di Zhang, Wei Liu, Qian Tan, Jingdan Chen, Hang Yan, Yuliang Yan, Jiatong Li, Weiran Huang, Xiangyu Yue, Dongzhan Zhou, Shufei Zhang, Mao Su, Hansen Zhong, Yuqiang Li, and Wanli Ouyang. Chemllm: A chemical large language model. *arXiv preprint arXiv:2402.06852*, 2024. URL <https://arxiv.org/abs/2402.06852>.
- Gengmo Zhou, Zhifeng Gao, Qiankun Ding, Hang Zheng, Hongteng Xu, Zhewei Wei, Linfeng Zhang, and Guolin Ke. Uni-mol: A universal 3d molecular representation learning framework. In *International Conference on Learning Representations (ICLR)*, 2023. URL <https://openreview.net/forum?id=6K2RM6wVqKu>.

A Proofs for Pointwise Squared Loss and CRPS

In this section, we formalize the difference between pointwise squared loss and CRPS at the population level. The key distinction is that pointwise squared loss evaluates a single prediction in isolation, whereas CRPS evaluates an entire predictive distribution.

A.1 Theoretical Comparison of Pointwise Squared Loss and CRPS

The two objectives induce different optimal solutions: squared loss is mean-seeking, while CRPS is distribution-seeking [Gneiting, 2011, Gneiting and Raftery, 2007, Matheson and Winkler, 1976]. These results are standard consequences of the Bayes optimality of squared loss for the conditional mean and the strict propriety of CRPS, but we restate them here to clarify the optimization bias induced by each objective in our multi-rollout regression setting.

Standard Result 1: Pointwise squared loss is mean-seeking. Fix an input x , and let $Y | X = x \sim P_x$ with finite second moment. Define the population pointwise squared-loss objective

$$\mathcal{L}_{\text{MSE}}(a; x) = \mathbb{E}[(a - Y)^2 | X = x], \quad a \in \mathbb{R}. \quad (6)$$

Then $\mathcal{L}_{\text{MSE}}(a; x)$ is uniquely minimized at

$$a^*(x) = \mu_x := \mathbb{E}[Y | X = x]. \quad (7)$$

Equivalently, among predictive distributions over scalar predictions, the minimizer of expected pointwise squared loss is the degenerate predictor δ_{μ_x} concentrated at the conditional mean [Gneiting, 2011].

Proof. Let $\mu_x = \mathbb{E}[Y | X = x]$. Expanding the square around μ_x gives

$$\mathcal{L}_{\text{MSE}}(a; x) = \mathbb{E}[(a - Y)^2 | X = x] \quad (8)$$

$$= \mathbb{E}[(a - \mu_x + \mu_x - Y)^2 | X = x] \quad (9)$$

$$= (a - \mu_x)^2 + 2(a - \mu_x)\mathbb{E}[\mu_x - Y | X = x] + \mathbb{E}[(\mu_x - Y)^2 | X = x]. \quad (10)$$

Since $\mathbb{E}[\mu_x - Y | X = x] = 0$, this simplifies to

$$\mathcal{L}_{\text{MSE}}(a; x) = (a - \mu_x)^2 + \text{Var}(Y | X = x). \quad (11)$$

The variance term does not depend on a , so the unique minimizer is $a = \mu_x$.

Now consider a predictive distribution F over scalar predictions \hat{Y} . If the model is evaluated by pointwise squared loss on a single sampled prediction $\hat{Y} \sim F$, then the population objective becomes

$$\mathbb{E}_{\hat{Y} \sim F} \mathbb{E}[(\hat{Y} - Y)^2 | X = x] = \mathbb{E}_{\hat{Y} \sim F} \left[(\hat{Y} - \mu_x)^2 + \text{Var}(Y | X = x) \right] \quad (12)$$

$$= \mathbb{E}_{\hat{Y} \sim F} [(\hat{Y} - \mu_x)^2] + \text{Var}(Y | X = x). \quad (13)$$

This is minimized by placing all mass at μ_x , namely $F = \delta_{\mu_x}$. Therefore, under pointwise squared loss, any predictive spread away from the conditional mean strictly increases the objective. This establishes that pointwise squared loss is inherently mean-seeking and favors collapse to a point mass, which is empirically verified in our analysis.

Standard Result 2: CRPS is distribution-seeking. Fix an input x , and let $Y | X = x \sim P_x$. For any predictive distribution F on \mathbb{R} with finite first moment, define

$$\mathcal{L}_{\text{CRPS}}(F; x) = \mathbb{E}_{Y \sim P_x} [\text{CRPS}(F, Y)]. \quad (14)$$

Then $\mathcal{L}_{\text{CRPS}}(F; x)$ is minimized at $F = P_x$. In particular, if P_x is non-degenerate, then for any point mass δ_a ,

$$\mathcal{L}_{\text{CRPS}}(P_x; x) < \mathcal{L}_{\text{CRPS}}(\delta_a; x). \quad (15)$$

Hence, when $\text{Var}(Y | X = x) > 0$, collapse to any single point, including the conditional mean, is suboptimal under CRPS [Matheson and Winkler, 1976, Gneiting and Raftery, 2007].

Proof. CRPS is a strictly proper scoring rule for univariate predictive distributions [Matheson and Winkler, 1976, Gneiting and Raftery, 2007]. Therefore, for any true conditional distribution P_x and any predictive distribution F with finite first moment,

$$\mathbb{E}_{Y \sim P_x} [\text{CRPS}(P_x, Y)] \leq \mathbb{E}_{Y \sim P_x} [\text{CRPS}(F, Y)], \quad (16)$$

with equality if and only if $F = P_x$.

This immediately proves the first claim: the population CRPS objective is minimized by the true conditional predictive distribution.

For the second claim, suppose P_x is non-degenerate. Then $P_x \neq \delta_a$ for every $a \in \mathbb{R}$. By strict propriety of CRPS, any predictive distribution different from P_x must incur strictly larger expected CRPS. In particular,

$$\mathcal{L}_{\text{CRPS}}(P_x; x) < \mathcal{L}_{\text{CRPS}}(\delta_a; x) \quad \text{for all } a \in \mathbb{R}. \quad (17)$$

Applying this to $a = \mu_x = \mathbb{E}[Y \mid X = x]$ shows that the mean-collapsed predictor δ_{μ_x} is strictly suboptimal whenever the conditional target distribution has nonzero spread.

Thus, unlike pointwise squared loss, CRPS does not reward collapse to a single point. Instead, it is optimized by the full conditional distribution.

A.2 Implication

The two standard results above formalize the contrast between pointwise and distributional regression objectives at the population level. Pointwise squared loss treats each prediction independently and is optimized by the conditional mean, so it provides no incentive to represent predictive uncertainty. In contrast, CRPS is a strictly proper scoring rule for predictive distributions and is optimized by the true conditional predictive law when that law is observed through repeated samples.

This population-level result motivates CRPS as a distribution-aware scoring rule. In our finite-sample LLM setting, however, DAR does not directly observe the full conditional distribution for each input. Instead, it uses the empirical negated CRPS against the available scalar target as a reward over multiple sampled rollouts. Thus, DAR should be viewed as a practical distribution-aware credit-assignment objective that encourages well-centered and appropriately dispersed rollout sets, rather than as a guarantee of recovering the true conditional distribution.

B Experimental Setup

In this section, we provide additional details on the experimental setup for the synthetic benchmark and the two real-world regression datasets, as well as the implementation details and baseline methods.

B.1 Tasks

Synthetic Distributional Regression. We construct a synthetic 1D distributional regression benchmark following Appendix E.2 of Fishkov et al. [2025]. For each input $x \in \mathbb{R}$, the ground-truth conditional distribution is a heteroscedastic two-component mixture:

$$p^*(y \mid x) = \pi(x)P_1(y \mid x) + (1 - \pi(x))P_2(y \mid x). \quad (18)$$

The input-dependent mixing weight is defined as

$$\pi(x) = \frac{1}{1 + \exp(1.2x)}, \quad (19)$$

and the two component means are given by

$$\mu_1(x) = \frac{x}{3} + 1.2 \sin(0.8x), \quad (20)$$

$$\mu_2(x) = \frac{x}{3} - 1.2 \cos(0.8x). \quad (21)$$

The input-dependent noise scale is

$$\sigma(x) = 0.12 + 0.28 (0.5 + 0.5 \sin(0.7x))^2. \quad (22)$$

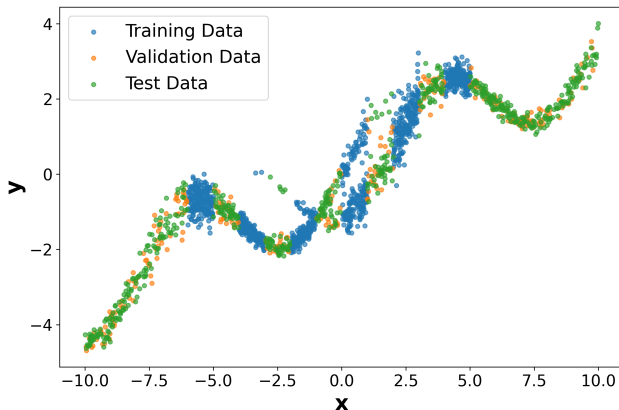


Figure 5: Illustration of data samples

Each component is Gaussian with shared heteroscedastic variance:

$$P_1(y | x) = \mathcal{N}(y; \mu_1(x), \sigma^2(x)), \quad (23)$$

$$P_2(y | x) = \mathcal{N}(y; \mu_2(x), \sigma^2(x)). \quad (24)$$

Equivalently, one may sample from the distribution via

$$k \sim \text{Bernoulli}(\pi(x)), \quad (25)$$

$$\epsilon \sim \mathcal{N}(0, 1), \quad (26)$$

$$y = \mu_k(x) + \epsilon \sigma(x). \quad (27)$$

Following the same setup, we draw $n = 1200$ training pairs (x, y) from $p^*(y | x)$. In our implementation, training inputs are sampled from the in-domain interval $x \in [-6, 6]$, while the test set covers both the training region and additional disjoint regions outside $[-6, 6]$ in order to evaluate both interpolation and extrapolation behavior. Figure 5 shows the one-dimensional distribution of the data samples.

Coding Performance Prediction. For code performance prediction, we use the akhauriyash/Code-Regression benchmark and restrict attention to the APPS and LEET portions.⁴ Following Akhauri et al. [2025], we construct random train/validation/test splits over these subsets. We adopt this protocol because the original authors do not provide an official fixed split for these data, and thus the random-split setup is consistent with their experimental practice. The task is to predict a continuous execution-related target from code alone, and our evaluation follows the standard regression setting used in prior work. The released dataset card specifies an MIT license for the packaged benchmark.

MoleculeNet Property Prediction. For molecular property prediction, we use the MoleculeNet benchmark [Wu et al., 2018] and focus on the three commonly used physicochemical regression subsets: ESOL, FreeSolv, and Lipophilicity (Lipo). MoleculeNet explicitly includes these regression tasks and recommends scaffold-based evaluation for such chemistry benchmarks, which is also the protocol commonly followed in recent work [Zhou et al., 2023, Yu et al., 2024]. In line with prior molecular representation work, including Uni-Mol and subsequent studies, we use the official scaffold split for ESOL, FreeSolv, and Lipo.

Regarding licensing, MoleculeNet is a benchmark that aggregates public molecular datasets, while the DeepChem software commonly used to access these benchmark tasks is released under the MIT License. Since ESOL, FreeSolv, and Lipophilicity originate from public source datasets collected into the MoleculeNet benchmark, usage should also respect the terms of the original underlying sources in addition to the benchmark software license. This benchmark structure is documented in MoleculeNet and related dataset documentation.

⁴The Hugging Face dataset card lists the dataset license as MIT.

Category	Value
Framework	ver1
Training method	GRPO
Train batch size	256
Learning rate	1×10^{-6}
PPO mini-batch size	16
PPO micro-batch size / GPU	4
Entropy coefficient	0
Use KL loss	True
KL loss coefficient	0.001
KL loss type	low_var_kl
Use KL in reward	False
Rollout engine	vLLM
Rollouts per prompt (n)	12
Sampling temperature	1.0
Top- p	1.0
Rollout GPU memory utilization	0.8
Rollout log-prob micro-batch size / GPU	8
Reference log-prob micro-batch size / GPU	8
Gradient checkpointing	True
Parameter offload	False
Optimizer offload	False
Critic warmup	0
GPUs	4
Nodes	1

Table 3: Main RL hyperparameters for DAR training in ver1. Our method follows the standard GRPO pipeline and differs mainly in the reward computation.

B.2 Baselines

For zero-shot evaluation of domain-specific language models, we follow the default generation protocol described in each original paper [Fang et al., 2023, Zhang et al., 2024, Yu et al., 2024]. For ICL [Vacareanu et al., 2024], we use 50 in-context examples for MoleculeNet property prediction and 10 for coding regression due to context length constraints. Following the original setup, these examples are randomly sampled from the training set.

For the value-head baseline, we follow the embedding-based regression setup of Tang et al. [2024]. Specifically, we keep the language model frozen and train only a lightweight prediction head on top of fixed input representations. For each example, we extract a fixed-dimensional embedding from the prompt field using a pretrained Qwen instruction model, and use this embedding as input to a two-hidden-layer MLP regressor with ReLU activations. The regression head is trained with mean squared error (MSE) on normalized target values, where the normalization statistics are computed only from the training split. At evaluation time, predictions are transformed back to the original target scale before computing all regression metrics. We optimize the regressor with AdamW, select the best checkpoint based on validation performance, and use early stopping with a maximum of 300 training steps. Overall, this setup closely follows the protocol of Tang et al. [2024].

For both SFT and RL training, we use the default training configuration provided in the ver1 repository. We keep the batch size and the number of training steps the same across methods for fair comparison.

B.3 Computing Resources

We use a single node with 4 H100 GPUs for all SFT and RL training runs. Depending on the model scale and the maximum number of training steps, each run takes approximately 1–2 days. Our method does not introduce additional computational overhead relative to the pointwise GRPO baseline.

Model	Reasoning	Zero-shot			DAR (ESOL)		
		# Tokens	ρ (\uparrow)	RMSE (\downarrow)	# Tokens	ρ (\uparrow)	RMSE (\downarrow)
Qwen3-4B	No	1072	0.67	1.62	7	0.90	0.73
Qwen3-4B	Yes	2737	0.66	1.68	2584	0.87	1.01

Table 4: ESOL regression results with and without explicit reasoning. We report the average number of output tokens, Spearman correlation (ρ), and RMSE for zero-shot and DAR.

B.4 Implementation Details

The Table 3 shows the detailed setup of the training. We implement both supervised fine-tuning (SFT) and reinforcement learning (RL) using the `verl`⁵ framework. For RL, we build on the standard GRPO training pipeline and replace only the reward computation with our distribution-aware reward. Concretely, for each prompt, the policy generates multiple rollouts, and our reward manager computes rollout-level rewards based on each sample’s contribution to the predictive distribution induced by the full rollout set. This design requires no additional value head, no auxiliary uncertainty head, and no extra learned scorer beyond the standard policy/reference setup.

Our method introduces only minimal computational overhead relative to standard GRPO. The dominant training cost remains rollout generation and policy optimization, which are unchanged. The additional cost comes only from reward-side aggregation over the sampled rollouts for each prompt. In practice, this is lightweight compared to model forward passes, since it operates on scalar predictions after decoding rather than on token-level hidden states. Thus, the training pipeline, hardware footprint, and optimization procedure remain nearly identical to standard GRPO. We trained each model on each dataset for sufficiently long training, up to a maximum of 400 steps, selected the best checkpoint based on validation performance, and then reported the final results on the test set.

C Reasoning Mode vs. Non-Reasoning Mode

On-policy RL is naturally compatible with reasoning-oriented models because it can reinforce longer intermediate derivations. We nevertheless disable explicit reasoning by default in our main experiments for efficiency, and instead study its effect through separate ablations in both the zero-shot and RL fine-tuning settings. In these ablations, we explicitly instruct the model in the system prompt to reason before producing a prediction, and set the maximum output length to 8192 during training.

Table 4 presents a controlled comparison on ESOL using Qwen3-4B-Instruct, evaluating both Reasoning=Yes and Reasoning=No under two settings: (i) zero-shot inference and (ii) DAR fine-tuning on ESOL. The results show that explicitly prompting the model to generate intermediate reasoning [Wei et al., 2022] substantially increases the number of output tokens, but does not improve regression performance in either setting. In the fine-tuning case, reasoning is in fact associated with worse performance. This trend is consistent with recent findings in GRPO training for verifiable tasks, which suggest that RL-based reasoning training can reduce output diversity [He et al., 2025, Petrenko et al., 2026]. A similar effect may be present here, as the reasoning-enabled model exhibits lower variance than the non-reasoning counterpart (total variance 3.5 vs. 4.2). Note that this finding is specific to our single-task fine-tuning setup on ESOL with small scale model, where training and evaluation are performed on the same task. It does not rule out the possibility that explicit reasoning could help in broader settings such as multi-task post-training or transfer.

D Predictive Distributional Evaluation with Proper Scoring Rules

We report CRPS and WIS [Bracher et al., 2021] to evaluate the quality of the predictive distribution. Both metrics are proper scoring rules, where lower values indicate better calibrated and sharper predictive distributions. As shown in Table 5, DAR generally achieves the best or competitive scores across the five datasets. In particular, DAR consistently improves over the MSE reward baseline on both CRPS and WIS, suggesting that directly shaping the predictive distribution is more effective than optimizing pointwise accuracy alone. Compared with SFT, DAR also achieves better scores on

⁵<https://github.com/verl-project/verl>

Dataset	Metric	SFT	MSE	DAR
KBSS	CRPS	0.306802	0.410821	0.338585
	WIS	0.319435	0.413349	0.348008
APPS	CRPS	0.070761	0.071566	0.069917
	WIS	0.071614	0.071624	0.069949
ESOL	CRPS	0.307318	0.296201	0.279290
	WIS	0.312944	0.300977	0.287004
FreeSolv	CRPS	0.460140	0.477857	0.419609
	WIS	0.464905	0.480833	0.424840
Lipo	CRPS	0.505357	0.560613	0.497898
	WIS	0.518844	0.564648	0.505950

Table 5: CRPS and WIS results across datasets for SFT, MSE, and DAR. Lower values indicate better predictive distribution quality.

APPS, ESOL, FreeSolv, and Lipo, while remaining competitive on KBSS. These results indicate that distribution-aware reward shaping improves predictive distribution quality by assigning appropriate probability mass around the ground-truth value without making the prediction intervals unnecessarily wide.

E Limitations

Comparison to traditional regression methods. While our results suggest that LLM-based regression can be useful for scientific prediction tasks, this approach also has important limitations relative to traditional nonlinear regression methods. Classical models such as Gaussian processes, kernel methods, gradient-boosted trees, and neural regression models are often more computationally efficient, easier to train, and better suited when the input is already available as structured numerical or tabular features. They also provide clearer inductive biases and, in some cases, more established uncertainty estimates. In contrast, LLM-based regression requires substantially more compute, depends on careful prompting and decoding choices, and may be less sample-efficient when the task does not benefit from language-based representations.

Flexibility and sensitivity. The main advantage of LLM-based regression is its flexibility: the same model can consume heterogeneous inputs such as natural-language descriptions, code, SMILES strings, metadata, or task specifications without task-specific feature engineering. This makes it attractive for settings where the input is naturally textual or where constructing specialized features is costly. However, this flexibility also introduces additional sources of variability. Predictions can be sensitive to prompt format, sampling temperature, output parsing, and the choice of backbone model. Moreover, although our distribution-aware objective improves rollout diversity and calibration, it does not eliminate all failure modes of RL training, such as unstable optimization, reward misspecification, or distribution shift between training and evaluation.

Scope of evaluation. Finally, our evaluation focuses on scalar regression tasks and predictive distributions formed from multiple sampled rollouts. Extending the method to higher-dimensional outputs, structured scientific predictions, or settings requiring strict physical constraints remains future work. Our results should therefore be interpreted as evidence that distribution-aware RL can improve LLM-based regression in the studied settings, rather than as a replacement for well-established regression methods in all domains.

F Broader Impact

LLM-based regression has the potential to support scientific domains where prediction targets are continuous quantities and inputs are heterogeneous, such as natural-language descriptions, code, molecular strings, metadata, or experimental conditions. By improving the quality of predictive

distributions, our work aims to provide a foundation for using LLMs not only as text generators, but also as flexible regression models for scientific prediction. This could help accelerate early-stage screening, experiment prioritization, and inverse-design workflows, where researchers need to reason about both expected outcomes and uncertainty before committing costly experimental or computational resources.

At the same time, these models should be used as decision-support tools rather than replacements for domain expertise or empirical validation. In scientific settings, inaccurate predictions or poorly calibrated uncertainty estimates could lead to wasted resources or misleading conclusions, especially in high-stakes areas such as materials discovery, drug development, or engineering design. Therefore, outputs from LLM-based regression systems should be interpreted cautiously, validated with domain-specific methods, and accompanied by uncertainty estimates when used for downstream decision making.

More broadly, we view this work as an initial step toward general-purpose scientific regression with language models. While the current study focuses on scalar prediction tasks, future extensions could support more complex inverse-engineering and design problems, where models propose or evaluate candidate systems under uncertainty. Responsible use will require careful benchmarking, transparent reporting of failure modes, and safeguards against over-reliance on model predictions.

G LLM Usage

LLMs are the primary model class studied in this work for regression with sampled predictive distributions. In addition, we used LLM-based tools to assist with grammar checking, wording refinement, and figure-generation code during manuscript preparation.

H Task Prompts

We present the system prompts and user instruction prompts used for each task. For all tasks, the target value is a single real number.

Note. The prompt boxes below show the exact system and instruction templates used in our experiments.

H.1 Synthetic Distributional Regression

System Prompt.

```
Given a synthetic regression sample, predict the target value y.
The input x is generated from a synthetic benchmark.
Output your estimate in \boxed{}. Only place the numeric value inside
the \boxed{}.
```

Instruction Prompt Template.

```
Synthetic regression task.
Input feature:
x = {x}

Predict the target value y.
```

Example.

```
Synthetic regression task.
Input feature:
x = 1.23456789
```

Predict the target value y .

H.2 Coding Performance Prediction

APPS System Prompt.

Given an APPS sample, predict the peak memory usage in bytes. Output your estimate in `\boxed{}`. Only place the numeric value inside the `\boxed{}`.

KBSS System Prompt.

Given a KBSS sample, predict the kernel execution latency in milliseconds. Output your estimate in `\boxed{}`. Only place the numeric value inside the `\boxed{}`.

Instruction Prompt Template. The instruction prompt is taken directly from the input field:

```
{code/problem context from the dataset input field}
```

Example Structure.

```
[Problem description, code snippet, or execution context from the dataset]
```

H.3 MoleculeNet Property Prediction

ESOL System Prompt.

Given a SMILES string, predict the aqueous solubility ($\log S$). Output your estimate in `\boxed{}`. Only place the numeric value inside the `\boxed{}`.

FreeSolv System Prompt.

Given a SMILES string, predict the hydration free energy in kcal/mol. Output your estimate in `\boxed{}`. Only place the numeric value inside the `\boxed{}`.

Lipo System Prompt.

Given a SMILES string, predict the octanol/water partition coefficient. Output your estimate in `\boxed{}`. Only place the numeric value inside the `\boxed{}`.

Instruction Prompt Template. The user prompt wraps the input molecule as a SMILES string:

```
<SMILES> {smiles_string} </SMILES>
```

Example.

```
<SMILES> CC(=O)OC1=CC=CC=C1C(=O)O </SMILES>
```